

1 Generalized angularities and differential jet shapes 2 measurements from STAR at $\sqrt{s} = 200$ GeV

3 **Tanmay Pani^{a,*} (for the STAR collaboration)**

4 ^a*Rutgers University,*

5 *136 Frelinghuysen Road, Piscataway, USA*

6 *E-mail: tp543@physics.rutgers.edu*

Jets from early stages of heavy-ion collisions undergo modified showering in quark-gluon plasma (QGP) relative to vacuum due to jet-medium interactions, which can be measured using observables like differential jet shape and generalized angularities. Differential jet shape ($\rho(\mathbf{r})$) encodes radially differential information about jet broadening and has shown an average migration of charged energy away from the axes of quenched jets from Pb+Pb collisions at the LHC. Measurements of generalized angularities in presence of the medium from Pb+Pb collisions at the LHC show harder, or more quark-like jet fragmentation relative to vacuum. Measuring these distributions in heavy-ion collisions at RHIC will help us further characterize jet-medium interactions in a phase-space region complementary to that of the LHC.

In these proceedings, we present the first fully corrected measurements of $\rho(\mathbf{r})$, jet girth (g), momentum dispersion (p_T^D) and momentum difference of leading and subleading constituent particles (LeSub) observables, using hard-core jets in $p + p$ collisions at $\sqrt{s} = 200$ GeV, collected by the STAR experiment. Finally, the data are compared with model calculations and the physics implications are discussed.

26-31 March 2023

Aschaffenburg, Germany

*Speaker

8 1. Introduction

9 Hard scattered partons from early stages of high-energy hadron collisions undergo successive,
 10 small-angle fragmentations, and eventually appear in the final state as collimated sprays of hadrons
 11 called *jets*. In heavy-ion collisions, jets traverse the quark-gluon plasma (QGP) medium and are
 12 modified relative to a $p + p$ baseline. This is known as *jet quenching* [1]. Therefore, jets are used
 13 as probes of QGP, containing information of interaction between hard partons and QGP medium.
 14 One way to access the quenching information is by studying intra-jet angular distribution of energy
 15 relative to the jet-axis through generalized jet angularities, calculated as:

$$\lambda_{\beta}^{\kappa} = \sum_{\text{const} \in \text{jet}} \left(\frac{p_{T,\text{const}}}{p_{T,\text{jet}}} \right)^{\kappa} r(\text{const}, \text{jet})^{\beta}, \quad (1)$$

16 where $p_{T,\text{jet}}$ is the jet's total momentum, and $r(\text{const}, \text{jet}) = \sqrt{(\eta_{\text{jet}} - \eta_{\text{const}})^2 + (\phi_{\text{jet}} - \phi_{\text{const}})^2}$
 17 is the (η, ϕ) distance of a constituent from the jet-axis. Parameters κ and β tune experimental
 18 sensitivity to hard and wide-angle radiation, respectively. λ_{β}^1 's are infra-red and collinear (IRC)
 19 safe angularities [2], which probe the average angular spread of energy around the jet-axis. They are
 20 radial moments of the jet's momentum profile, also known as differential jet-shape ($\rho(\mathbf{r})$), given by,

$$\rho(\mathbf{r}) = \lim_{\delta r \rightarrow 0} \left\langle \frac{1}{\delta r} \frac{\sum_{|\mathbf{r}_{\text{const}} - \mathbf{r}| < \delta r/2} p_{T,\text{const}}}{p_{T,\text{jet}}} \right\rangle_{\text{jets}}, \quad (2)$$

21 where $\mathbf{r}_{\text{const}} = (\eta_{\text{const}} - \eta_{\text{jet}})\hat{\eta} + (\phi_{\text{const}} - \phi_{\text{jet}})\hat{\phi}$, and it follows that,

$$\lambda_{\beta}^1 = \int_{\text{jet}} r^{\beta} \rho(\mathbf{r}) d\mathbf{r}. \quad (3)$$

22 The jet angularity based observables like jet-substructure measurements in Pb+Pb collisions
 23 at $\sqrt{s_{\text{NN}}} = 2.76$ TeV at the LHC, have shown quenched jets, on average, have migration of charged
 24 energy away from their axis relative to a $p + p$ baseline [3] and possibly a survivor bias toward
 25 harder, quark-like fragmentation [4]. Similar measurements using jets with lower $p_{T,\text{jet}}$ at RHIC,
 26 will help understand jet-medium interactions in a complementary phase-space region to LHC.

27 In this proceeding, jet girth ($g = \lambda_1^1$), momentum dispersion ($p_T^D = \sqrt{\lambda_0^2}$) and the differential
 28 jet-shape ($\rho(\mathbf{r})$) are measured in $p + p$ collisions $\sqrt{s} = 200$ GeV to set a baseline for heavy-ion
 29 collisions at RHIC. We also calculate a non-angularity based jet observable LeSub which gives a
 30 measure of the hardest splitting of the jet:

$$LeSub = p_{T,\text{constituent}}^{\text{leading}} - p_{T,\text{constituent}}^{\text{subleading}}. \quad (4)$$

31 2. Dataset and Analysis Method

32 The analysis uses data from $p + p$ collisions at $\sqrt{s} = 200$ GeV collected in 2012 using
 33 the Solenoidal Tracker At RHIC (STAR) detector system. Charged-particle tracks and neutral
 34 energy depositions (towers) are measured using STAR's Time Projection Chamber (TPC) [5] and
 35 Barrel Electromagnetic Calorimeter (BEMC) [6] detectors respectively. Together, they provide
 36 full azimuthal coverage with a pseudorapidity acceptance of $|\eta| \leq 1$. The tracks and towers are

clustered into jets using the anti- k_T algorithm with a jet resolution parameter $R = 0.4$, implemented using the FastJet library [7]. To suppress contributions of fake tracks and combinatorial background (especially in the context of the larger heavy-ion background), a “hard-core” constituent selection as was done in previous STAR analyses [8] is applied, which only allows tracks (towers) with $c p_{T,\text{track}}(E_{T,\text{tower}}) \geq 2$ GeV to be clustered into jets. To enhance jet signal, only High-Tower (HT) triggered events, with at least one tower with $E_{T,\text{tower}} \geq 4$ GeV are considered. After clustering, only jets completely falling within acceptance ($|\eta_{\text{jet}}| \leq 0.6$) are kept. Jets with area, $A_{\text{jet}} < 0.3$ are rejected to further reduce the fake jet contribution.

The distributions of g , p_T^D and LeSub are fully corrected for detector effects by using iterative bayesian unfolding, implemented using the RooUnfold library [9]. The unfolding requires a response matrix between particle-level and detector-level. This is constructed using an embedding simulation which involves PYTHIA-6 STAR tune [10] events processed into detector hits using GEANT3 [11] and added to real zero-bias events from $p + p$ collision environment. To calculate $\rho(\mathbf{r})$, additional associated tracks not clustered into jets, but inside the jet cones are also used. This was done to look at the complete jet, around its hard core. Given a jet, tracks with $p_{T,\text{assoc}} \geq 1$ GeV/ c and $r(\text{assoc}, \text{jet}) \leq 0.4$ are used. The $\rho(\mathbf{r})$ is corrected using bin-by-bin factors obtained from the aforementioned embedding simulation¹.

3. Result and Discussion

Differential jet-shape as a function of $r = r(\text{assoc}, \text{jet})$ from the jet axis is shown in Fig. 1. Girth (g), p_T^D and LeSub distributions are shown in Fig. 2. Systematic uncertainties are shown as shaded grey bands. On average, lower energy jets with $15 \leq p_{T,\text{jet}} < 20$ GeV/ c have higher g , lower $LeSub$ and more energy away from jet-axis than jets with $p_{T,\text{jet}} \geq 20$ GeV/ c .

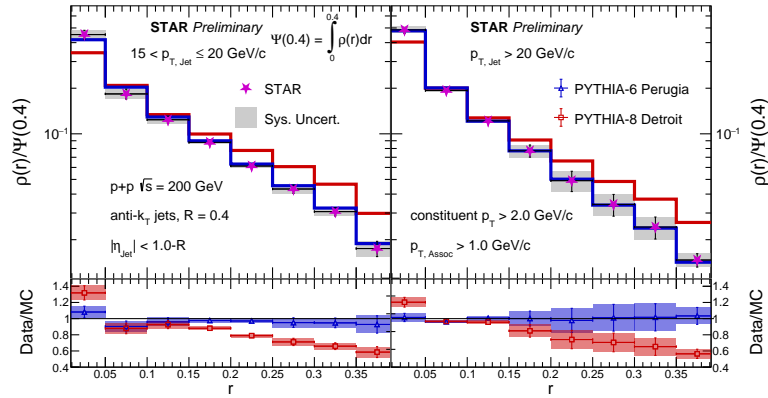


Figure 1: $\rho(\mathbf{r})$ vs r (magenta stars, normalized to unity) for jets with $15 \leq p_{T,\text{jet}} < 20$ GeV/ c (left) and $p_{T,\text{jet}} \geq 20$ GeV/ c (right). The results are compared to PYTHIA-6 (STAR) (blue) and PYTHIA-8 (Detroit) (red). The lower panels show the ratio of the data calculation to the PYTHIA-6 (STAR) (blue) and PYTHIA-8 (Detroit) (red).

¹Details of closure associated with the unfolding can be found in slides 25-33 in the talk associated with this proceeding, <https://www.indico.uni-muenster.de/event/1409/contributions/2038/attachments/859/1764/HP2023.pdf>

59 The results are compared to PYTHIA-6 (STAR) [10] and PYTHIA-8 Detroit underlying event
 60 tune [12]. All measurements show a good agreement with PYTHIA-6, while PYTHIA-8 is shown
 61 to underestimate jets with higher $LeSub$ and lower g values. $\rho(\mathbf{r})$ from PYTHIA-8 underestimates
 62 the fraction of jet momentum closer to the jet axis. Figures 3 and 4 show STAR data compared to
 63 PYTHIA-8 (Detroit) with (a) all hard scatterings, (b) only $qq \rightarrow qq$ hard scatterings (quark jets),
 64 and (c) only $gg \rightarrow gg$ hard scatterings (gluon jets).

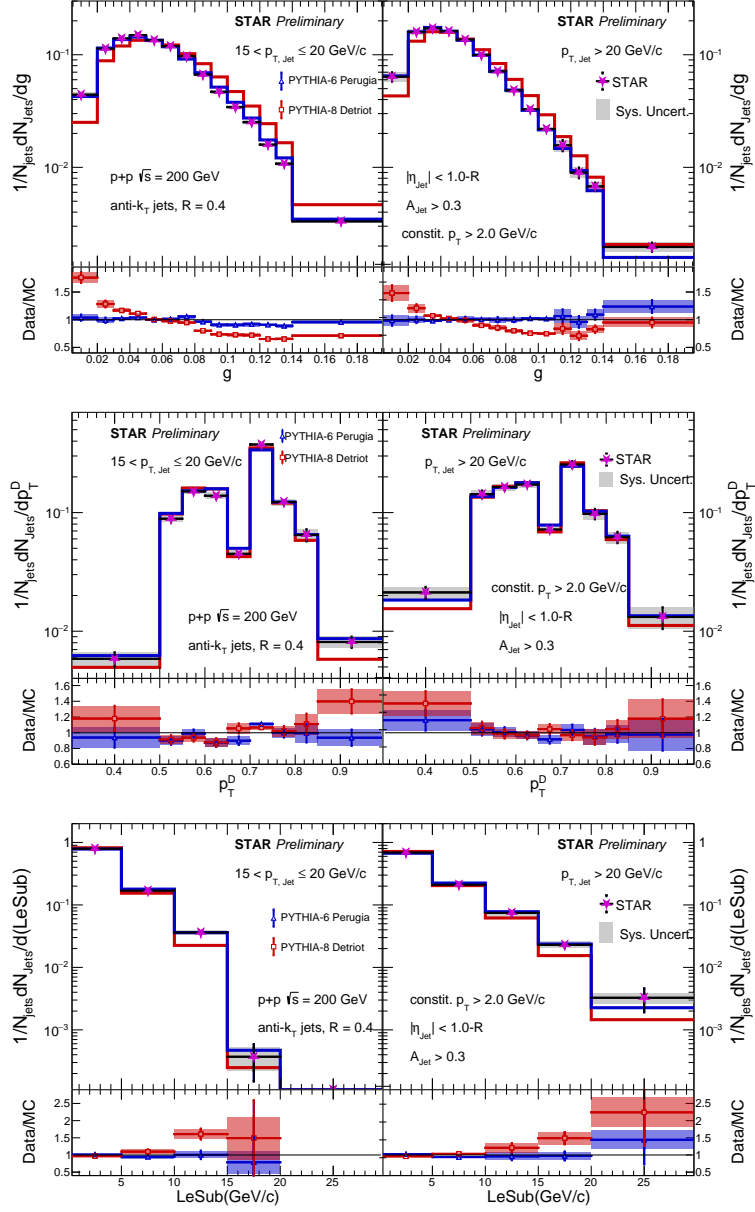


Figure 2: g (top), p_T^D (middle) and $LeSub$ (bottom) distributions (magenta stars, normalized to unity) for jets with $15 \leq p_{T,jet} < 20$ GeV/c (left) and $p_{T,jet} \geq 20$ GeV/c (right). The results are compared to PYTHIA-6 (STAR) (blue) and PYTHIA-8 (Detroit) (red). The lower panels show the ratio of the data calculation to the PYTHIA-6 (STAR) (blue) and PYTHIA-8 (Detroit) (red).

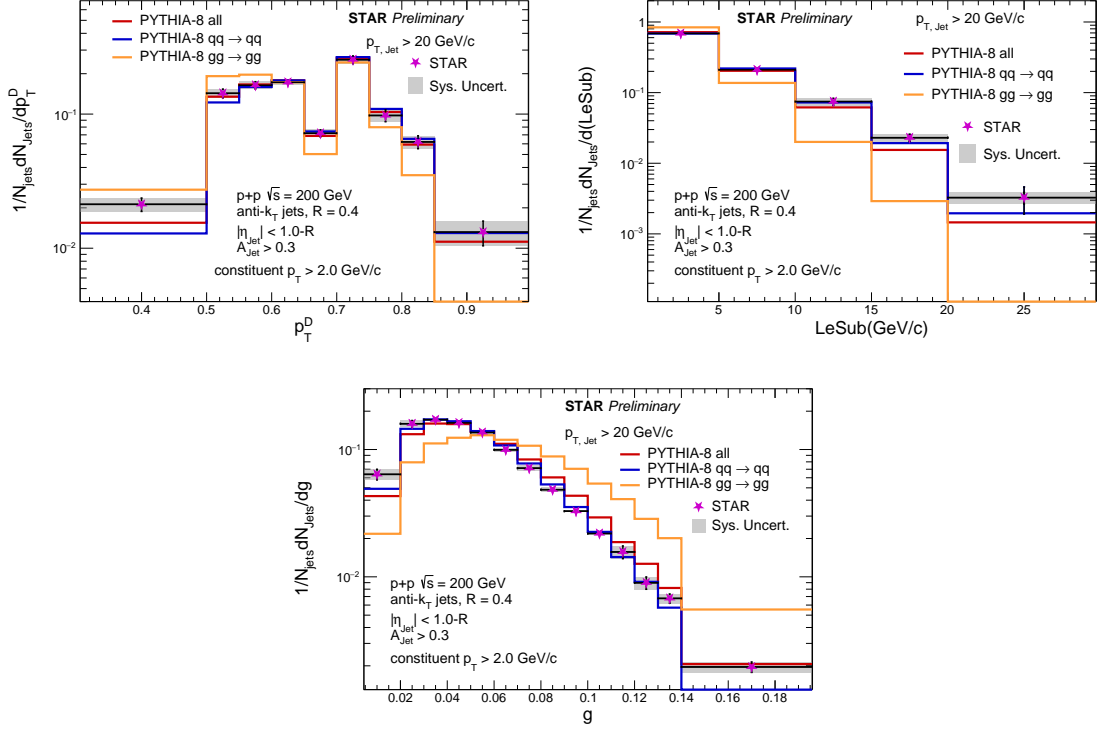


Figure 3: $p_T^D = \sqrt{\lambda_0^2}$ (top-left), LeSub (top-right) and g (bottom) distributions for jets with $p_{T,\text{jet}} \geq 20$ GeV/c. The results are compared to PYTHIA 8 (Detroit) with all hard processes (red), with only $qq \rightarrow qq$ processes (blue) and $gg \rightarrow gg$ processes (orange).

65 Since gluon jets have softer, more spread-out radiation pattern on average than quark jets [13],
 66 they are likely to have lower p_T^D , lower LeSub , higher g with more momentum ($\rho(\mathbf{r})$) away from the
 67 jet-axis. As even quark-jets from PYTHIA-8 (Detroit) show softer fragmentation on average than
 68 the STAR data, it is likely that PYTHIA-8 (Detroit) underestimates hard fragmentation of partons.

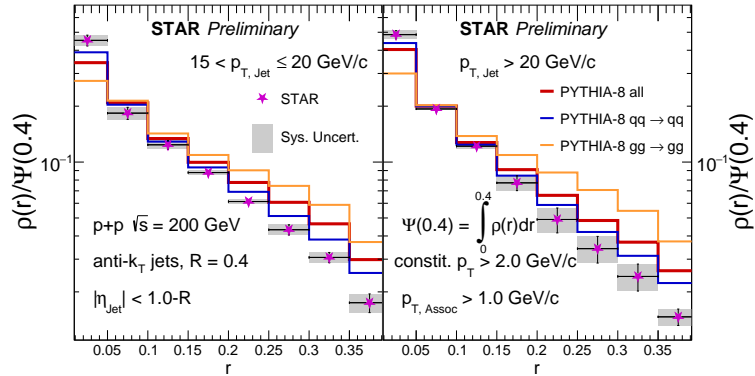


Figure 4: $\rho(r)$ vs r (magenta) for $15 \leq p_{T,\text{jet}} < 20$ GeV/c (left) and $p_{T,\text{jet}} \geq 20$ GeV/c (right). The results are compared to PYTHIA 8 (Detroit) with all hard processes (red), with only $qq \rightarrow qq$ processes (blue) and $gg \rightarrow gg$ processes (orange).

4. Conclusions

First measurements of jet-shape observables g , p_T^D , LeSub and $\rho(\mathbf{r})$ from STAR using hard-core jets $p + p$ collisions at $\sqrt{s} = 200$ GeV are presented, setting the baseline for heavy-ion collisions to measure the medium-modification at RHIC. With the hard-core jet definition and HT trigger requirement, the sample of jets used here is biased towards hard-fragmented jets. The results show good agreement with PYTHIA-6 (STAR). PYTHIA-8 (Detroit) is shown to underestimate harder-fragmented jets, and needs further tuning of PYTHIA-8's parton shower/hadronization parameters to explain STAR hard-core jets.

This work is supported by the National Science Foundation under Grant number: 1913624.

References

- [1] M. Gyulassy, I. Vitev, X.-N. Wang and B.-W. Zhang, *Jet quenching and radiative energy loss in dense nuclear matter*, in *Quark–Gluon Plasma 3*, pp. 123–191, World scientific (2004).
- [2] A.J. Larkoski, J. Thaler and W.J. Waalewijn, *Gaining (mutual) information about quark/gluon discrimination*, *Journal of High Energy Physics* **2014** (2014) .
- [3] S. Chatrchyan et al., *Modification of jet shapes in PbPb collisions at $\sqrt{s_{NN}} = 2.76$ TeV*, *Physics Letters B* **730** (2014) 243.
- [4] S. Acharya et al., *Medium modification of the shape of small-radius jets in central Pb-Pb collisions at 2.76 TeV*, *Journal of High Energy Physics* **2018** (2018) .
- [5] M. Anderson et al., *The STAR time projection chamber: a unique tool for studying high multiplicity events at RHIC*, *Nuc. Inst. and Methods in Physics Research* **499** (2003) 659.
- [6] M. Beddo et al., *The STAR barrel electromagnetic calorimeter*, *Nuc. Inst. and Methods in Physics Research* **499** (2003) 725.
- [7] M. Cacciari, G.P. Salam and G. Soyez, *FastJet user manual*, *The European Physical Journal C* **72** (2012) .
- [8] STAR collaboration, *Differential measurements of jet substructure and partonic energy loss in Au+Au collisions at $\sqrt{s_{NN}} = 200$ GeV*, *Phys. Rev. C* **105** (2022) 044906.
- [9] L. Brenner et al., *Comparison of unfolding methods using RooFitUnfold*, *International Journal of Modern Physics A* **35** (2020) 2050145.
- [10] J.K. Adkins, Ph.D. thesis, University of Kentucky, 2019. [arXiv/1907.11233](https://arxiv.org/abs/1907.11233).
- [11] R. Brun et al., *GEANT3*, CERN-DD-EE-84-1.
- [12] M.R. Aguilar et al., *Pythia8 underlying event tune for RHIC energies*, *Phys. Rev. D* **105** (2022) 016011.
- [13] J. Gallicchio and M.D. Schwartz, *Quark and gluon tagging at the LHC*, *Physical Review Letters* **107** (2011) .